Energy Transfer between Polyatomic Molecules. 1. Gateway Modes, Energy Transfer Quantities and Energy Transfer Probability Density Functions in Benzene−Benzene and Ar−Benzene Collisions†

V. Bernshtein and I. Oref*

Department of Chemistry, Technion-Israel institute of Technology, Haifa 32000, Israel

Received: July 26, 2004; In Final Form: December 5, 2004

We report collisional energy transfer, CET, quantities for polyatomic−polyatomic collisions and use excited benzene collisions with cold benzene bath, B−B, as our sample system and compare our results with the CET of excited benzene with Ar bath. We find that the gateway mode for both systems is the out-of-plane modes and that in B−B CET, vibration to vibration, V−V, is the dominant channel. Rotations play a mechanistic role in the CET but the net rotational energy transfer is small compared to V−V. The shape of the down side of the energy transfer probability density function, $P(E,E')$, is convex for B−B collisions and it becomes less so as the temperature increases. In Ar−B collisions, $P(E,E')$ is concave and it becomes less so as the temperature decreases. We report average vibrational, rotational, and translational energy transferred, $\langle\Delta E\rangle$, as function of temperature for various initial conditions.

Introduction

Collisional energy transfer (CET) between molecules is the mechanism by which activation/deactivation in reactive, photochemical, and photophysical processes in the gas phase takes place. Because of its major importance, a great deal of experimental and theoretical effort went into exploring various facets of the subject. With the availability of cheap and powerful computational facilities in the last twenty years, classical trajectory calculations on various aspects of reactive and nonreactive systems in the gas-phase came into maturity. The majority of the computational efforts went into calculating CET parameters for excited polyatomic molecules-inert bath gases systems[1−29] with few studies on di-, tri-, and polyatomic bath gases.[30−33] Despite the great importance of energy transfer between highly excited polyatomic molecules and polyatomic bath gas to reactive, photochemical and photophysical processes, not enough computational effort was spent on this subject and the present work is devoted to some aspects of it.

Trajectory calculations of CET between highly excited polyatomic molecules and inert gases[1] indicate that the major mode of energy transfer is vibration to rotation to translation, V−R−T. Rotations are the mechanism by which vibrational energy is converted to translational energy in the process of activation/deactivation.[21] The average collision duration of such collisions is short and no correlation was found between the collision duration and the average amount of energy transferred, $\langle\Delta E\rangle$.[27] This happens because the actual energy transfer occurs in a short "kick" of about 50 fs at the end of the collision complex lifetime after which the bath atom departs.[14,15] The gateway modes in collisions of excited benzene and Ar are the low lying out-of-plane, OOP, vibrations. In a series of calculations we have found[26] that if OOP and in-plane, IP, vibrations have the same frequency the OOP is more effective in transferring energy but if the IP vibrations have lower frequencies than the OOP then, the IP are the most effective. Thus the most important factor is frequency followed by the dynamic geometry of the modes, OOP being more effective than the IP.

In polyatomic−polyatomic collisions the situation is different. Lenzer and Luther, LL, in their work on excited benzene−benzene CET[30] and Grigoleit et al.[32] on excited pyrazine-*n*-propane found that the most efficient channel of CET is V−V transfer. What appears to be different from collision with monatomic bath is not the existence of the V−V channel (it does not exist in inert bath) but the fact that, according to LL, rotations almost do not play a role in the CET, contrary to the situation with inert bath gas. In the work below we explore the mechanism of CET between an excited polyatomic and a polyatomic bath. We address the questions of, what are the gateway modes, the average collision duration, $\langle\tau\rangle$, the correlation between $\langle\tau\rangle$ and the average energy transferred in a collision, $\langle\Delta E\rangle$? We evaluate the intermolecular energy transfer probability density function $P(E,E')$ and finally, we compare the results of polyatomic−polyatomic collisions with those of polyatomic-inert bath.

Theory

The numerical methods used in the present work are reported in refs 14 and 15. The equations of motion are integrated by using a modified computer program Venus.[34] The intermolecular potential is pairwise Lennard-Jones. The details of the potential are reported in refs 13 and 18. The intramolecular potential includes all the normal mode contributions, stretching, bending and wagging. The values of the parameters of this potential were obtained from the modified valence force field calculations by Draeger and are also given in refs 14 and 15. Normal-mode analysis gave good agreement with experimental values. The modes are reported in Table 1. The initial translational and rotational energies were chosen from the appropriate thermal energy distributions. The initial impact parameter was chosen randomly from values between 0 and its maximum value b_m. The value of the maximum impact parameter b_m was determined separately. A value of 1.3 nm was used in the present

† Part of the special issue "George W. Flynn Festschrift".

* Corresponding author. E-mail: chroref@technion.ac.il.

10.1021/jp046693d CCC: $30.25
Published on Web 02/10/2005

TABLE 1: Normal and Modified Modes of Benzene Used in the Calculations (Frequencies in cm^{-1})[a]

	mode frequency					
standard	IP ↔ OOP swapped	IP → OOP	OOP → IP	OOP frozen	IP frozen	type of motion
400.3*2	616.9 *2		616.9 *2	669.4*2		OOP
616.8*2	400.1*2	400.1*2			1064.1*2	IP
657.3	928.9		928.9	949.4		OOP
680.0						OOP
832.7*2	1251.6*2		1251.6*2	7636.3*2		OOP
926.4						IP
991.1*2	972.6*2	972.6*2			1238.5*2	IP
1014.6*2	1699.6*2		1699.6*2	11747.5*2		OOP
1025.9	643.2	643.2			13231.0	IP
1070.3	1955.3		1955.3	14347.3		OOP
1133.5*2	1123.4*2	1123.4*2			1394.4*2	IP
1173.0						IP
1375.4						IP
1530.5*2	1515.3*2	1515.3*2			4906.3*2	IP
1739.1*2	1693.5*2	1693.5*2			10516.8*2	IP
1749.4						IP
3056.6*2						IP
3056.7	3052.5*2	3052.5*2				IP
3059.0*2	3055.7*2	3055.7*2				IP
3060.1	3049.6	3049.6				IP

[a] IP, in-plane modes; OOP, out-of-plane modes. *2 indicates 2-fold degenerate mode.

calculations. The initial internal energy was an assigned value. The collision duration was determined by monitoring the beginning and the end of each collision by the forward and backward sensing (FOBS) method.[14,15,29] In the FOBS method a collision is defined by a change ϵ in the internal energy of the excited molecule in a time interval Δt. After careful and exhaustive study, Δt was determined to be 10 fs and the ratio $\epsilon/\Delta t$ was taken to be 0.35 and 3.5 cm^{-1}/fs.

In the frequency shuffling runs, the torsion and bending force constants of the OOP and/or IP modes where changed to give the desired frequencies. Table 1 gives the original frequencies from normal-mode analysis and the new frequencies after changes were made in the appropriate force constants. In one set of calculations (IP → OOP) the 617 cm^{-1} frequency of the IP mode was assigned the same frequency as the 400 cm^{-1} OOP mode and the 1056 cm^{-1} IP mode was assigned the frequency of 643 cm^{-1}, very similar to the OOP frequency of 657 cm^{-1}. In another set of calculations, the OOP modes where given the values of IP modes. A total of five frequencies, belonging to eight modes, three of whom are degenerate, were changed and are listed in Table 1.

In yet another set of calculations in this series, frequencies were exchanged. The frequency of the IP modes were changed to the lowest frequencies of the OOP modes and the OOP modes were assigned the frequencies of the IP modes. In some calculations, a subset of modes was frozen so as not to allow exchange of energy with the environment. This was done by increasing the values of some of the force constants, which caused a few-fold increase in the frequencies whose modes we wished to freeze. These frequencies are also given in Table 1. A total of 50 000 trajectories were used for each set of initial conditions. The large number of trajectories was chosen to provide good statistical sampling in the binning process.

Results and Discussion

The purpose of the present work is to gain insight into the detailed mechanism of CET between polyatomic molecules and to compare the results with those for CET between polyatomic molecules and inert gases. To this end we have investigated CET between a series of hot and cold benzene molecules. The results of the computations are given below.

Energy Transfer Quantities in Benzene−Benzene Collisions. In studying benzene−benzene (B−B) collisions, a B molecule was excited to 40 700 cm^{-1}, and denoted by B*. This value of the excitation energy was used previously in experimental[40] and in computational work.[30] The bath B molecules were at kept at constant temperature in the range 200−500 K. The detailed results of the calculations for 300 K, which amounts to 370 cm^{-1} of internal thermal energy of the cold bath molecule, are summarized in Table 2. Column 1 shows the CET values for the native system of B* colliding with B. As can be seen, the major contribution to $\langle\Delta E\rangle$ is V−V CET whereas rotations, which participate in the mechanism of CET, do not transfer rotational energy. These results support the B*−B CET findings of LL[30] that V−V is the major channel of CET but disagree with their statement that rotations are not important. As can be seen from the table, even though $\langle\Delta E_R\rangle_a$ is only −17 cm^{-1}, compared with $\langle\Delta E\rangle_a$ of −755 cm^{-1}, the values of $\langle\Delta E_R\rangle_d$ and $\langle\Delta E_R\rangle_u$ are respectively −173 and +143 cm^{-1}. Our interpretation of these large values is that rotations play a role in the CET even though their net contribution to the overall value of $\langle\Delta E\rangle_a$ is insignificant. An examination of animations of trajectories also shows that rotations take indeed an active part in CET. Translational CET, exactly as rotational CET, is not very large: $\langle\Delta E_T\rangle_a$ being 33 cm^{-1} at 200 K and 50 cm^{-1} at 500 K. The up and down average CET quantities are larger: at 500 K $\langle\Delta E_T\rangle_d$ = 210 cm^{-1} and $\langle\Delta E_T\rangle_d$ = 257 cm^{-1}. A check for conservation of energy shows that the cold bath B molecule gained whatever B* lost, as expected.

Column 2 shows the CET results when the IP and the OOP frequencies are swapped in both B. The value of $\langle\Delta E\rangle_a$ decreased by 300 cm^{-1} compared to the value of the native system shown in column 1, and the deficiency all came from a decrease in the value of average vibrational energy transferred in a down collision $\langle\Delta E_V\rangle_d$. However, there is no marked change in the rotational energy transfer and the average collision duration, $\langle\Delta\tau\rangle$, has changed by only 10%. All these indicate that the OOP modes are the gateway modes for CET. This conclusion is supported by the results in columns 3 and 6. Column 3 shows the results for the case when the IP 617 and 1026 cm^{-1} modes are assigned, in both B, the OOP modes frequencies 400 and 643 cm^{-1}. There is no change in the CET values compared with

TABLE 2: Benzene−Benzene Collisions (Excited Benzene $E_v^A = 40\,700$ cm^{-1}; Cold Benzene $E_v^B = 370$ cm^{-1}; $T = 300$ K; $\langle \Delta E \rangle$ in cm^{-1}; τ_{coll} in ps; $\epsilon/\Delta t = 0.35$ cm^{-1}/fs)[a]

	1	2	3	4	5	6	7	8	9	10	11
$\langle \Delta E \rangle_a$[b]	−755	−476	−763	−766	−766	−467	−363	−293	−488	−524	−709
$\langle \Delta E \rangle_d$	−906	−620	−911	−920	−917	−607	−505	−434	−622	−678	−858
$\langle \Delta E \rangle_u$	61	89	58	60	66	95	120	131	109	115	97
$\langle \Delta E_V \rangle_a$	−739	−453	−750	−752	−746	−440	−334	−257	−454	−513	−685
$\langle \Delta E_V \rangle_d$	−855	−555	−860	−867	−866	−532	−432	−341	−537	−624	−795
$\langle \Delta E_V \rangle_u$	49	70	46	50	48	51	66	66	51	77	59
$\langle \Delta E_R \rangle_a$	−17	−23	−13	−14	−20	−27	−29	−35	−34	−11	−24
$\langle \Delta E_R \rangle_d$	−173	−186	−174	−175	−175	−180	−185	−190	−192	−184	−186
$\langle \Delta E_R \rangle_u$	149	152	155	153	147	145	148	152	155	167	158
$\langle \tau_{coll} \rangle_a$	2.13	2.20	2.07	2.10	2.11	2.21	1.86	1.75	1.88	1.83	1.84
$\langle \tau_{coll} \rangle_d$	2.28	2.38	2.21	2.25	2.24	2.38	2.01	1.86	2.02	1.94	1.95
$\langle \tau_{coll} \rangle_u$	1.33	1.50	1.29	1.29	1.35	1.52	1.34	1.40	1.29	1.37	1.25

[a] Numbers: 1, normal vibrations; 2, IP and OOP vibrations swapped in both benzenes; 3, IP is the same as OOP vibrations for both benzenes; 4, IP is the same as OOP vibrations in the excited benzene; 5, IP is the same as OOP vibrations in the cold benzene; 6, OOP is the same as IP vibrations for both benzenes; 7, OOP vibrations of both benzenes frozen; 8, OOP vibrations of both benzenes frozen; the internal energy is reduced by the energy that would have been in the frozen modes; 9, OOP vibrations of the excited benzene frozen; 10, OOP vibrations of the cold benzene frozen; 11, IP vibrations of both benzenes frozen. [b] Subscripts: a indicates all; u indicates up; d indicates down collision; V, vibrational energy; R, rotational energy. τ_{coll} is the collision lifetime.

TABLE 3: Benzene−Benzene Collisions (Initially Frozen Rotations ($T_R^{A,B} = 0$ K); $T_T^{A,B} = 300$ K; $T_V^B = 300$ K; $E_v^A = 40\,700$ cm^{-1}; $\langle \Delta E \rangle$ in cm^{-1}; τ_{coll} in ps; $\epsilon/\Delta t = 0.35$ cm^{-1}/fs)[a]

	1	2	3	4	5	6	7	8	9	10
$\langle \Delta E \rangle_a$[b]	−899	−720	−699	−951	−904	−904	−925	−395	−331	−790
$\langle \Delta E \rangle_d$	−1162	1041	−1035	−1208	−1175	−1158	−1188	−616	−545	−1017
$\langle \Delta E \rangle_u$	40	64	66	30	40	37	41	84	79	71
$\langle \Delta E_V \rangle_a$	−971	−786	−766	−1021	−976	−977	−998	−459	−392	−865
$\langle \Delta E_V \rangle_d$	−1102	−922	−914	−1149	−1108	−1105	−1134	−558	−479	−991
$\langle \Delta E_V \rangle_u$	19	22	27	12	20	20	21	40	35	42
$\langle \Delta E_R \rangle_a$	72	67	67	70	72	73	73	64	62	76
$\langle \Delta E_R \rangle_d$	0.0	0.0		0.0	0.0	0.0	0.0	0.0	0.0	0
$\langle \Delta E_R \rangle_u$	72	67	67	70	72	73	73	64	62	76
$\langle \tau_{coll} \rangle_a$	5.32	5.84	5.77	5.69	5.29	5.39	5.40	9.39	11.61	5.55
$\langle \tau_{coll} \rangle_d$	6.39	7.53	7.50	6.79	6.38	6.44	6.46	12.80	16.69	6.63
$\langle \tau_{coll} \rangle_u$	1.51	1.72	1.80	1.46	1.50	1.48	1.51	1.97	1.90	1.43

[a] Numbers: 1, normal vibrations; 2, OOP vibrations of both benzenes frozen; 3, OOP vibrations of the excited benzene frozen; 4, OOP of the cold benzene frozen; 5, IP is the same as OOP vibrations for both benzenes; 6, IP is the same as OOP vibrations for the excited benzene; 7, IP is the same as OOP vibrations for the cold benzene; 8, OOP vibrations of both benzenes frozen; 9, OOP vibrations of both benzenes frozen; the internal energy is reduced by the energy that would have been in the frozen modes; 10, IP vibrations of both benzenes frozen. [b] Subscripts: a indicates all; u indicates up; d indicates down collision; V, vibrational energy; R, rotational energy. τ_{coll} is the collision lifetime.

the original values of $\langle \Delta E \rangle$ in column 1, which supports the previous conclusion that the OOP modes are the gateway modes for CET. Assigning the IP modes the OOP frequencies in only one of the B's, as in columns 4 and 5, does not change the values of $\langle \Delta E \rangle$. However, when the OOP modes are assigned the values of the IP modes, in both B, the value of $\langle \Delta E_V \rangle$, shown in column 6, drops by 300 cm^{-1}, exactly as in column 2. This provides additional evidence of the importance of OOP modes to the CET and for the obvious conclusion that the lower the frequency of the OOP modes the higher the value of $\langle \Delta E_V \rangle$.

If the conclusion that was reached in the previous paragraph is correct, that the OOP modes are the key players in CET, then, "freezing" these modes selectively, e.g., changing their force constants in a way that increases significantly the frequencies of the modes and thus removing them from the CET process, should support this conclusion. Column 7 shows what happens when the OOP modes are frozen and the energy is distributed among the remaining modes. Column 8 is the same as 7 but the total energy distributed among the active modes is reduced by the amount that would have been in the OOP modes such that each active mode has the same energy it had when no mode was frozen. The value of $\langle \Delta E_V \rangle_d$ is reduced by 50% compared to the value of the native system! Although there is a dramatic change in the value of $\langle \Delta E_V \rangle$ when the OOP vibrations are altered, not much is happening to the values of rotational CET quantities. The value of $\langle \Delta E_R \rangle_d$ is almost the same as the value of $\langle \Delta E_R \rangle_u$, as befitting a thermal system, and the values are the same as in the native system described in column 1. Columns 9 and 10 give high-resolution information on the CET process. When the OOP modes of the excited B are frozen, the value of $\langle \Delta E \rangle_a$ is reduced by 260 cm^{-1}, to only 65% of the native system. When the OOP modes of the cold bath B are frozen, there is almost an identical reduction in $\langle \Delta E \rangle_a$ whereas the value of $\langle \Delta E_V \rangle_d$ is larger by 200 cm^{-1} than the value of $\langle \Delta E_V \rangle_d$ of the system in column 7, where the OOP of both B are frozen, and larger by 100 cm^{-1} than the value in column 9 where only the OOP modes of the excited B are frozen. Thus, between the two benzene molecules, the hot and the cold, the OOP modes of the cold B affect the least the transferring of energy. Freezing the IP modes of both B molecules, as in column 11, hardly affects the CET process. Everything so far points to the conclusion that the OOP modes are the major contributors to the CET process.

Table 3 shows CET values for the case where the rotations of each molecule are initially frozen. There are two items that stand out when Tables 2 and 3 are compared. The first is that $\langle \Delta E_V \rangle_d$ for the frozen rotations is larger, by as much as 30%, than the value of $\langle \Delta E_V \rangle_d$ when the rotations are not frozen. The second is that the average collision duration $\langle \tau \rangle_d$ is larger by more than a factor of 4 than the value of $\langle \tau \rangle_d$ for normal collisions. The two effects are tied to each other in the following way. In the absence of rotations, which tend to prevent the formation of a collision complex, the two B molecules form a collision complex with a much longer lifetime. This enables an

TABLE 4: Temperature Effects in Benzene−Benzene and Benzene−Argon Collisions (E_v^A = 40 700 cm^{-1}; $\epsilon/\Delta t$ = 3.5 cm^{-1}/fs; $\langle\Delta E\rangle$ in cm^{-1}; τ_{coll} in ps)[a]

	$\langle\Delta E\rangle_a$	$\langle\Delta E\rangle_d$	$\langle\Delta E\rangle_u$	$\langle\Delta E_V\rangle_a$	$\langle\Delta E_V\rangle_d$	$\langle\Delta E_V\rangle_u$	$\langle\Delta E_R\rangle_a$	$\langle\Delta E_R\rangle_d$	$\langle\Delta E_R\rangle_u$	$\langle\tau_{coll}\rangle_a$	$\langle\tau_{coll}\rangle_d$	$\langle\tau_{coll}\rangle_u$
Benzene−Benzene Collisions												
T = 200 K	−841	−944	37	−824	−904	31	−17	−129	108	3.078 (2.049)*	3.268 (2.115)	1.459 (0.623)
T = 250 K	−789	−915	49	−773	−870	38	−16	−152	130	2.520 (1.570)	2.687 (1.637)	1.401 (0.580)
T = 300 K	−755	−906	61	−739	−855	49	−17	−173	149	2.100 (1.239)	2.241 (1.302)	1.344 (0.561)
T = 500 K	−713	−994	141	−685	−910	120	−29	−261	213	1.437 (0.729)	1.523 (0.771)	1.177 (0.530)
Benzene−Argon Collisions												
T = 100 K	−57	−122	60	−84	−156	63	27	−72	105	4.989 (3.935)	5.234 (4.190)	4.546 (3.455)
T = 200 K	−44	−149	96	−43	−141	89	−1	−120	119	2.876 (2.034)	2.951 (2.091)	2.776 (1.954)
T = 300 K	−44	−182	123	−29	−143	107	−15	−160	139	1.991 (1.248)	2.015 (1.280)	1.962 (1.209)
T = 500 K	−53	−249	174	−21	−167	144	−32	−239	187	1.304 (0.693)	1.314 (0.690)	1.292 (0.695)

[a] E_v^A energy in the excited benzene. Subscripts: a indicates all; u indicates up; d indicates down collision; V, vibrational energy; R, rotational energy. τ_{coll} is the collision lifetime. Results in parenthesis are for FOBS 3.5 cm^{-1}/fs.

efficient V−V energy transfer and hence the large values of $\langle\Delta E_V\rangle_d$ for the case of frozen rotations. We conclude that even though very little rotational energy is transferred during the CET, rotations do play a mechanistic role in the CET by affecting the lifetime of the collision complex.

Comparing column 1 with 2−4 shows that freezing out the OOP vibration of the excited molecule reduces the value of $\langle\Delta E_V\rangle_d$ by as much as 200 cm^{-1} whereas freezing the OOP vibration of the cold bath molecule does not change the value of $\langle\Delta E_V\rangle_d$. This supports the conclusion that the gateway mode for CET is the OOP modes of the excited molecule. Columns 5−7 show that changing the frequencies of the IP to that of the OOP for either hot or cold molecule does not make any difference to the CET. However, as in Table 2, freezing the OOP vibrations reduces the value of $\langle\Delta E_V\rangle_d$ by ∼50% whereas increasing the collision lifetime by more than a factor of 2. This is clearly seen in columns 8 and 9. It appears that the increase in lifetime, which generally enhances CET in B−B, is not enough to compensate for the blocking of the OOP gateway modes. Column 10 shows that freezing the IP modes makes only little difference in the values of $\langle\Delta E_V\rangle_d$. This lends additional support to the conclusion that the OOP vibrations are the gateway modes for energy transfer.

Table 4 shows the effect of temperature on CET quantities. As can be seen, the magnitude of $\langle\Delta E\rangle_a$ decreases with an increase in temperature. This happens because $\langle\Delta E_V\rangle_u$ increases with an increase in translational energy whereas $\langle\Delta E_V\rangle_d$ is unaffected by it. It is the weighted sum of the two that actually cause the reduction in the value of $\langle\Delta E\rangle_a$. This reduction in $\langle\Delta E\rangle_a$ with an increase in temperature is accompanied by a marked reduction in the collision lifetime by as much as a factor of 2. This shows that the higher the average translational energy, the shorter the average collision duration and the higher the values of $\langle\Delta E_V\rangle_u$, $\langle\Delta E_R\rangle_d$, and $\langle\Delta E_R\rangle_u$. Because $\langle\Delta E_V\rangle_u$ is much smaller than $\langle\Delta E_V\rangle_d$, the overall effect is a change of only 20% in the value of $\langle\Delta E_V\rangle_a$, unlike B−Ar collisions where the change is a factor of 2.[23]

Mechanism of Energy Transfer between Two Benzene Molecules. We find that in B−B collisions there is a clear correlation between the lifetime of the collision complex and the amount of energy transferred, the longer the duration of the collision the larger is the average value of ΔE transferred. This is clearly seen in Figure 1a where the average energy transferred in a bin is plotted as a function of the collision duration. It should be

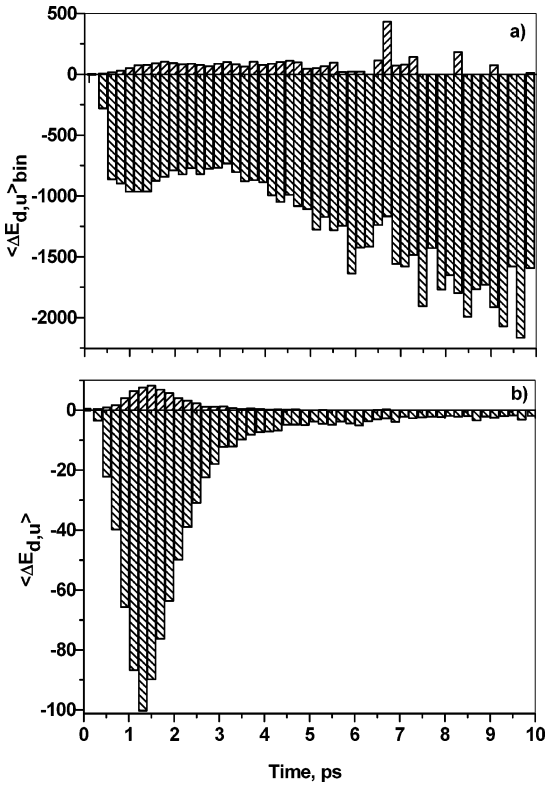

Figure 1. Histograms of $\langle\Delta E\rangle$ vs collision duration for benzene−benzene collisions. The excitation energy of the hot benzene is 40 700 cm^{-1} and the cold bath is at 300 K. The FOBS value is $\epsilon/\Delta t$ = 0.35 cm^{-1}/fs. (a) Average energy transferred in a given collision duration. (b) Values in (a) weighted by the probability of obtaining a collision of a given duration.

pointed out that the probability for collisions of long duration, longer than twice the value of $\langle\tau\rangle$, and for large ΔE, supercollision, is very small.[37] So, the actual amount of energy transferred by these, long-lived, collisions is small. This can be seen in Figure 1b where the histogram of Figure 1a is multiplied by the probability of obtaining a collision of a given duration. The contribution of the long-lived collisions is not very large but it has an effect. Eight percent of all collisions longer than twice the value of $\langle\Delta\tau\rangle$ transfer 12% of the energy, a quantity not to be ignored. This is unlike the case of Ar−B, where the collision duration is not correlated with ΔE and energy

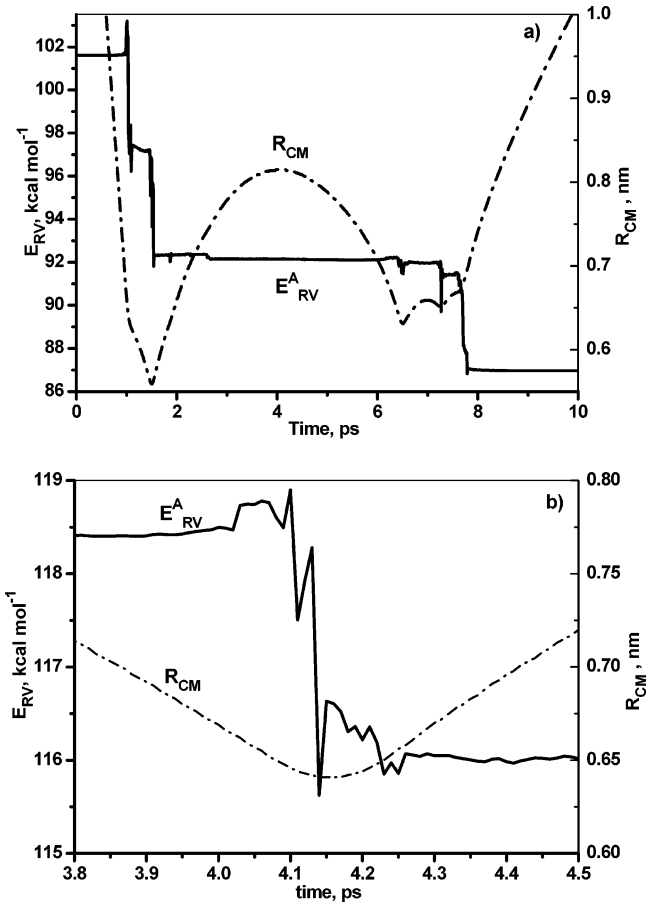

Figure 2. Two trajectories of excited benzene (40 700 cm^{-1})−benzene bath collisions at 300 K. R_{CM} indicates the center of mass distance. E^A_{RV} indicates the vibrational rotational energy of the excited benzene. (a) Long-lived, chattering collision that transfers a large quantity of energy, 5120 cm^{-1} (supercollision). (b) Short-lived, hit and run, collision which transfers energy equal to an out-of-plane vibration.

transfer takes place in the last 50 fs of the collision complex lifetime regardless of its duration.[14]

The two mechanisms of energy transfer taking place in short and long lifetime collisions, are demonstrated by two trajectories depicted in Figure 2. Figure 2a shows a long-lived trajectory of ∼7 ps of a supercollision[37] with $\Delta E = 5120$ cm^{-1}. This is an example of a chattering collision where every time the two molecules get close to each other energy is transferred. On the other hand, Figure 2b shows a short-lived collision where the two molecules approach each other and exchange energy in ∼30 fs. The peak to peak energy difference is 1050 cm^{-1}, which is the frequency of an OOP mode of a collisional period of 32 fs. Looking at the trajectory of the cold bath molecule (not shown) shows a gain of identical amount of energy in an identical time period. This is an example of pure resonance V−V transfer that occurs in one shot in one single approach.

Are the OOP modes the most efficient in CET? We have tried to answer that before for the B−Ar system, and we examined it here for the B−B system by selecting few initial orientations of the rotationally frozen colliding pairs while allowing for all impact parameters as in normal collisions. The results are given in Table 5. Comparing the values of the various $\langle\Delta E_V\rangle$'s in column 2 for collisions where the planes of the two B are parallel to each other and perpendicular to the direction of motion and the values in column 3 where the two B's approach each other on the same plane head on in the direction of motion with the values of $\langle\Delta E_V\rangle$ in normal, random collision, given in column 1, shows that these orientations contribute by

TABLE 5: Orientation Effect in Benzene−Benzene Collisions (Initially Frozen Rotations ($T_R^{A,B} = 0$ K); $T_T^{A,B} = 300$ K; $T_V^B = 300$ K; $E_v^A = 40\,700$ cm^{-1}; $\langle\Delta E\rangle$ in cm^{-1}; τ_{coll} in ps; $\epsilon/\Delta t = 0.35$ cm^{-1}/fs)[a]

	1	2	3	4	5
$\langle\Delta E\rangle_a$[b]	−899	−645	−643	−818	−891
$\langle\Delta E\rangle_d$	−1162	−840	−819	−1127	−1108
$\langle\Delta E\rangle_u$	40	33	34	43	47
$\langle\Delta E_V\rangle_a$	−971	−712	−701	−900	−963
$\langle\Delta E_V\rangle_d$	−1102	−824	−782	−1023	−1072
$\langle\Delta E_V\rangle_u$	19	23	15	9	22
$\langle\Delta E_R\rangle_a$	72	67	58	82	73
$\langle\Delta E_R\rangle_d$	0	0	0	0	0
$\langle\Delta E_R\rangle_u$	72	67	58	82	73
$\langle\tau_{coll}\rangle_a$	5.32	4.12	4.29	5.15	5.32
$\langle\tau_{coll}\rangle_d$	6.39	4.93	4.94	6.38	6.12
$\langle\tau_{coll}\rangle_u$	1.51	1.33	1.79	1.73	1.88

[a] Numbers: 1, normal, random collisions; 2, plane-to-plane; 3, in-plane, head-on; 4, Excited benzene perpendicular to collision direction and to the cold benzene; 5, cold benzene perpendicular to collision direction and to the excited benzene. [b] Subscripts: a indicates all; u indicates up; d indicates down collision; V, vibrational energy; R, rotational energy. τ_{coll} is the collision lifetime.

almost a third less to the values of $\langle\Delta E_V\rangle$. When the two B approach each other in a T orientation the CET quantities, in columns 4 and 5, are as large as those in column 1. The efficiency of the T shape approach in CET might be correlated with the fact that this configuration was found also to be stable in beam experiments.[36] This configuration is also very conductive to OOP CET. A plot of $\langle\Delta E\rangle$ for the T shape approach configuration vs impact parameter (not shown) shows that efficient CET occurs at all impact parameters within the collision sphere. For the in-plane head-on approach there are some intermediate impact parameters that are not conductive to CET whereas in the parallel approach all impact parameters are operational but the values of $\langle\Delta E_V\rangle$ are smaller.

Collisional Energy Transfer Probability Density Function. Interpreting kinetic data usually requires solving a master equation that requires, as part of the input data, CET probability density function, $P(E,E')$.[35] This quantity is hard to come by and various attempts were made to obtain it experimentally and thoretically.[35] Looking at the energy evolution in the excited molecule, Barker et al. used IR flourescence (IRF),[38−43] Troe et al. used UV absorption (UVA),[44−46] and Lenzer and Luther used kinetically controlled selective ionizations (KCSI)[47,48] as the experimental tool of choice. By using a complementary method, Flynn et al.[49−52] and Mullin et al.[53,54] have looked at the energy evolution in the colliding cold bath molecules. To interpret the results of the experiments, one has to solve an assumed master equation, with all the difficulties associated with it. The complexity of the system does not lend itself to be expressed by simple analytical models. Early models of CET by Rabinovitch, Oref, Tardy, and Nordholm, and co-workers are discussed in ref 35 and lately new attempts by Dashevskaya, Nikitin, and Oref[55−58] and Nordholm and co-workers[59] were made. However, a comprehensive model is yet to come.

Trajectory calculations, in addition for being very useful in providing CET quantities and shedding light on the mechanism of CET, can provide important information on $P(E,E')$. Not long ago we have developed a method by which we can calculate $P(E,E')$ directly from trajectory calculations without assuming a model.[23a] We do so by taking all effective collisions, collisions that cause a change in internal energy as defined by FOBS, including those with an elastic outcome, binning the values of $\langle\Delta E\rangle_{u,d}$, and normalizing it by the total number of effective collisions. In classical trajectory calculations a collision must

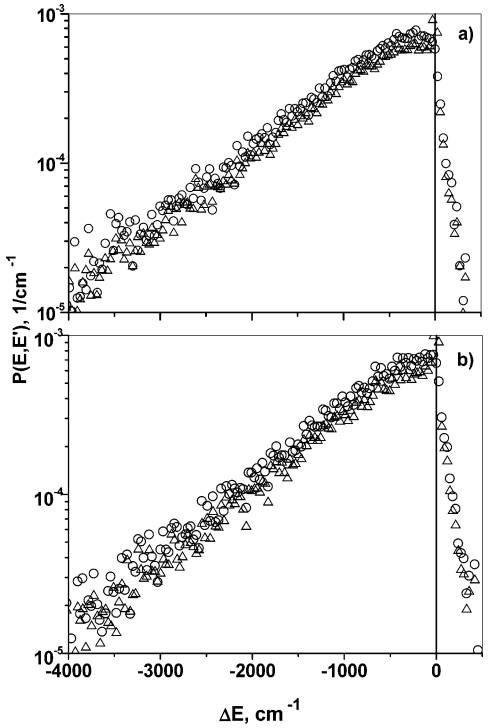

Figure 3. $P(E,E')$ of benzene−benzene bath collisions at (a) 200 K and (b) 250 K and two FOBS values. The excitation energy is 40 700 cm^{-1}. The triangles are points calculated with $\epsilon/\Delta t = 0.35$ cm^{-1}/fs and the circles with $\epsilon/\Delta t = 3.5$ cm^{-1}/fs. Note the progressive disappearance of convex shape of the data as the temperature increases.

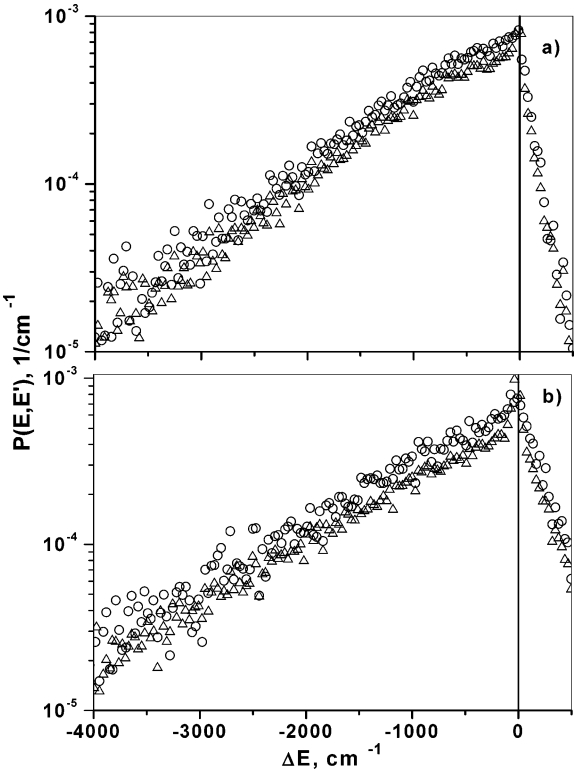

Figure 4. $P(E,E')$ of benzene−benzene bath collisions at (a) 300 K and (b) 500 K and two FOBS values. The excitation energy is 40 700 cm^{-1}. The triangles are points calculated with $\epsilon/\Delta t = 0.35$ cm^{-1}/fs and the circles with $\epsilon/\Delta t = 3.5$ cm^{-1}/fs. Note the progressive disappearance of convex shape of the data as the temperature increases.

be defined explicitly because not all trajectories can be defined as a collisional event. For example, a trajectory with a large impact parameter can describe a noncollisional event from the CET point of view and it is wrong to count it and use it in calculating $P(E,E')$. Therefore we use FOBS as our criterion for collisions. The essence of the FOBS method is to define a true collisional event by a change ϵ in the internal energy of the excited molecule in a time interval Δt. So, only trajectories that interact are counted, even though the event can turn out to be an elastic collision where no energy is exchanged. However, as discussed below, the method has its limitations. Once Δt is chosen to be 10 fs, there is a degree of arbitrariness in the choice of the value of ϵ. Therefore, to check the sensitivity of $P(E,E')$ to the numerical value of $\epsilon/\Delta t$, we have evaluated $P(E,E')$ by using the values 0.35 cm^{-1}/fs, chosen as the most appropriate value after detailed statistical analysis, and a value that is 10-fold larger, 3.5 cm^{-1}/fs.

The raw results of the calculations, with the FOBS values an order of magnitude apart, are shown in Figure 3 for B^* excited to 40 700 cm^{-1} in a B bath at (a) 200 K (b) 250 K and in Figure 4 at (a) 300 K and (b) 500 K. The triangles are points calculated with $\epsilon/\Delta t = 0.35$ cm^{-1}/fs and the circles with $\epsilon/\Delta t = 3.5$ cm^{-1}/fs. As can be seen, there is very good agreement between the circles and the triangle despite the large disparity in the FOBS value. As expected, the only significant difference between the two is around the $\Delta E = 0$ transition where the large value of $\epsilon/\Delta t = 3.5$ cm^{-1} washes out the small ΔE increments. $P(0,0)$ not withstanding, we are therefore confident that the method enables us to draw qualitative conclusions from overall trends exposed by the shape of $P(E,E')$.

One major qualitative conclusion is, in B−B collisions at low temperatures, 200 and 250 K, in the down collision part of $P(E,E')$ there is a distinct peak at values of ΔE smaller than 0. At 300 K it is still there but, it disappears at 500 K. The convex shape of the down collision part of $P(E,E')$ was discovered by LL and co-workers in KCSI experiments at 300 K,[47,48] and our calculations suggest that it is worthwhile to repeat the experiment at higher temperatures, if it is at all possible experimentally, to see whether the convex shape disappears as the temperature of the experiment is raised.

The calculational points in the up and down branches were also fitted by multiexponential functions[60,61]

$$P(E,E') = \sum_{i}^{n} [a_i \exp(-\Delta E/\alpha_i)] \qquad (1)$$

where n varies between 1 and 3 and a and α are fitting parameters. In addition, we have used stretched exponential fitting functions:

$$P(E,E') = \sum_{i}^{n} [a_i \exp((-\Delta E/\alpha_i))^{Y_i}] \qquad (2)$$

where n can be 1 or 2 and α and Y are fitting parameters. α depends also on the internal energy. Lenzer, Luther, and co-workers[48] have used identical equation but with $n = 1$.

We have fitted the trajectory results by using eqs 1 and 2 with n up to 2, or 3, depending on the equation. As can be recalled, the raw data, represented in Figures 3 and 4, for the two FOBS values are very similar except around $\Delta E = 0$ where the data for 0.35 cm^{-1}/fs is irregular and not amenable to smooth fitting. We could have, of course, ignored the points around $\Delta E = 0$ as was done in ref 33, but we felt that the data set is good enough and deserves to be treated as a whole. Figure 5 shows the data of $P(E,E')$ with the FOBS value of 3.5 cm^{-1}/fs and the weighted best fit to double exponential function

TABLE 6: Benzene−Argon Collisions (Excited Benzene $E_v^A = 40\ 700\ cm^{-1}$; $T = 300$ K; $\langle \Delta E \rangle$ in cm^{-1}; τ_{coll} in ps; $\epsilon/\Delta t = 0.35\ cm^{-1}/fs$)[a]

	1	2	3	4	5	6	7	8	9	10	11
$\langle \Delta E \rangle_a$[b]	−44	−32	−46	−26	−37	−27	−22	−24	−24	−19	−30
$\langle \Delta E \rangle_d$	−182	−165	−186	−155	−178	−165	−161	−172	−165	−165	−162
$\langle \Delta E \rangle_u$	123	126	128	124	134	130	130	141	135	137	124
$\langle \Delta E_V \rangle_a$	−29	−6	−39	7	−6	12	15	11	17	24	−1
$\langle \Delta E_V \rangle_d$	−143	−113	−160	−78	−108	−67	−58	−86	−67	−52	−110
$\langle \Delta E_V \rangle_u$	107	107	115	88	102	90	79	104	91	84	114
$\langle \Delta E_R \rangle_a$	−15	−26	−8	−33	−31	−39	−38	−35	−41	−44	−29
$\langle \Delta E_R \rangle_d$	−160	−169	−162	−160	−171	−175	−165	−173	−172	−176	−171
$\langle \Delta E_R \rangle_u$	139	133	151	119	136	125	119	132	125	123	135
$\langle \tau_{coll} \rangle_a$	1.99	2.12	1.96	2.14	1.85	2.00	2.01	1.96	1.99	1.88	2.59
$\langle \tau_{coll} \rangle_d$	2.02	2.09	1.97	2.12	1.86	1.85	1.90	1.96	1.92	1.72	2.67
$\langle \tau_{coll} \rangle_u$	1.96	2.16	1.96	2.17	1.84	2.17	2.12	1.97	2.07	2.05	2.51

[a] Numbers: 1, normal vibrations; 2, IP and OOP vibrations swapped; 3, IP is the same as OOP vibrations; 4, OOP is the same as IP vibrations; 5, IP vibrations frozen; 6, OOP vibrations frozen; 7, IP and OOP vibrations frozen; 8, IP vibrations frozen; the internal energy is reduced by the energy that would have been in the frozen modes; 9, OOP vibrations frozen; the internal energy is reduced by the energy that would have been in the frozen modes; 10, IP and OOP vibrations frozen; the internal energy is reduced by the energy that would have been in the frozen modes; 11, IP and OOP vibrations swapped; Ar has a mass of benzene. [b] Subscripts: a indicates all; u indicates up; d indicates down collision; V, vibrational energy; R, rotational energy; τ, collision lifetime.

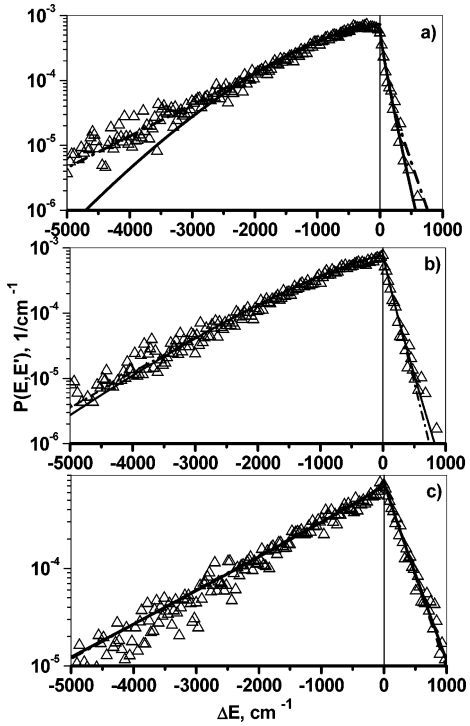

Figure 5. $P(E,E')$ of excited benzene collisions with benzene bath molecules (a) 200 K, (b) 300 K, and (c) 500 K. The FOBS value is $\epsilon/\Delta t = 3.5\ cm^{-1}/fs$. The excitation energy is 40 700 cm^{-1}. Shown are the best fit to double exponential, eq 1 (− · −), and stretched exponential, eq 2 with $n = 1$ (—).

described by eq 1 and to the stretched exponential given by eq 2 with $n = 1$. Separate fits were done to up collisions and down collisions. We have chosen to show only these functions because no additional insight is gained by higher order fit and the extra lines simply clutter the figures. As can be seen from this figure, the fit to both equations is good. We have performed two independent conservation-relation checks on the quality of our fit. We have integrated the fitting functions between the limits of $-\infty \leq \Delta E \leq \infty$ and found that for FOBS 0.35 cm^{-1}/fs the area at 300 K is unity ±11% and for FOBS 3.5 cm^{-1}/fs it is unity ±2%. We also evaluated $\langle \Delta E \rangle_{a,d,u}$ at 300 K by integrating $\int P(E,E')_{a,d,u} \Delta E_{a,d,u}\, d\Delta E$ over all values of ΔE. Here the double exponential value gave the original value less 5%, an excellent agreement. The LL equation gave poor agreement. This is probably due to deviations at high values of ΔE. A double exponential function was found by Barker et al.[62] to fit the IRF experiments on pyrazine-pyrazine collisions where a substantial supercollision tail was found.

Although the conservation relations are obeyed and the fitting goodness is $R^2 > 0.98$ we do not report the fitting parameter because they depend somewhat on the FOBS value of $\epsilon/\Delta t$. However, in any FOBS value we used, our qualitative conclusions are the same: the value of Y is larger than unity for low temperatures (convex lines) and its value decreases with an increase in temperature. As an example, at $\epsilon/\Delta t = 3.5\ cm^{-1}/fs$: at 200 K $Y = 1.56$ whereas at 500 K $Y = 0.96$. Absolute values notwithstanding, the trend is clear and it is also observed in Ar−B collisions which are discussed later. LL have taken $Y > 1$ to indicate polyatomic−polyatomic collisions. However, our results indicate that this is true only at low temperatures and it is entirely possible that if experiments are performed at high temperatures it will be found that $Y < 1$. In Figure 8 of the trajectory calculations of Higgins and Chapman's on the pyrazine−CO system,[33] $P(E,E')$ is given for four values of the translational energy, which can represent roughly the average temperature of the system. Their figure shows that the higher the translational energy the more concave is the line, in full agreement with our findings. Not only Y depends on the temperature, but also α decreases with temperature. α is defined by LL as an energy dependent parameter: $\alpha = C + C_1(E)$. It is probably related to $\langle \Delta E \rangle_a$ and, as can be seen from Table 4, this quantity decreases with temperature. (This is expected because, as the temperature increases, $\langle \Delta E_V \rangle_{d,u}$ increases but the weighted average of the two, $\langle \Delta E \rangle_a$, decreases until it approaches zero at thermal equilibrium when the up and down collisions transfer equal amounts of average energy. This trend agrees with the experimental results of Barker et al. on pyrazine−pyrazine collisions.[62])

*Energy Transfer Quantities in Benz*ene*−Ar Collisions.* It is of great interest to compare the CET mechanism and energy transfer quantities in polyatomic−polyatomic collisions with those of polyatomic-monatomic collisions and we have chosen the Ar/B system as a prototype of the latter. We have published extensively on the Ar/B system,[21−23,25−27] and in the following we will draw on previous work and report here only new computational results, which were performed under identical conditions to those of the B−B system. Column 1 in Table 6 shows the various CET quantities under normal conditions at 300 K. Swapping the IP with the OOP vibrations as in column

TABLE 7: Initially Frozen Rotations in Benzene−Argon Collisions (T_R = 0 K; T_T = 300 K; E_v = 40 700 cm^{-1}; $\langle\Delta E\rangle$ in cm^{-1}; τ_{coll} in ps; $\epsilon/\Delta t$ = 0.35 cm^{-1}/fs)[a]

	1	2	3	4
$\langle\Delta E\rangle_a$[b]	61	94	95	112
$\langle\Delta E\rangle_d$	−106	−60	−42	−14
$\langle\Delta E\rangle_u$	115	127	116	118
$\langle\Delta E_V\rangle_a$	−36	3	12	31
$\langle\Delta E_V\rangle_d$	−124	−70	−42	−12
$\langle\Delta E_V\rangle_u$	67	68	55	46
$\langle\Delta E_R\rangle_a$	97	91	82	81
$\langle\Delta E_R\rangle_d$	0	0	0	0
$\langle\Delta E_R\rangle_u$	97	91	82	81
$\langle\tau_{coll}\rangle_a$	3.65	5.15	5.59	7.25
$\langle\tau_{coll}\rangle_d$	5.86	9.27	12.12	22.52
$\langle\tau_{coll}\rangle_u$	2.94	4.25	4.58	6.56

[a] Numbers: 1, normal vibrations; 2, IP vibrations frozen; 3, OOP vibrations frozen; 4, IP and OOP vibrations frozen. [b] Subscripts: a indicates all; u indicates up; d indicates down collision; V, vibrational energy; R, rotational energy; τ, collision lifetime.

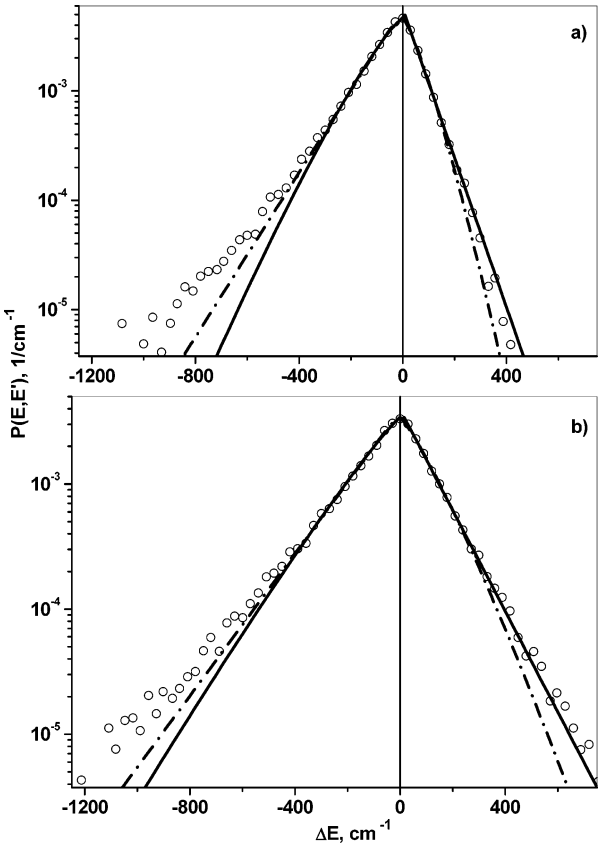

Figure 6. $P(E,E')$ of benzene−Ar collisions at (a) 100 K and (b) 200 K and $\epsilon/\Delta t$ = 3.5 cm^{-1}/fs. The excitation energy is 40 700 cm^{-1}. Shown are the best fit to double exponential, eq 1 (− · −), and stretched exponential, eq 2 with n = 1 (—). The lines become progressively more concave.

2 causes a ∼20% reduction in the value of $\langle\Delta E_V\rangle_d$. However, comparing column 3 to 1 shows that changing the IP frequencies to those of the OOP causes an increase of ∼12% in the values of $\langle\Delta E_V\rangle_d$, that is to say, reducing the frequencies of the IP modes increases the efficiency of energy transfer. If, on the other hand, column 4, where the OOP is changed to the IP frequencies, is compared to column 1, the efficiency of CET, judging from the value $\langle\Delta E_V\rangle_d$, drops by 45%! So, increasing the gateway frequency has a large effect on CET. With all the changes in columns 2−4, the values of $\langle\Delta E_R\rangle_d$ do not change whereas the value of $\langle\Delta E_R\rangle_u$ is affected somewhat by the changes. Although up and down rotational energy transfer quantities are larger than

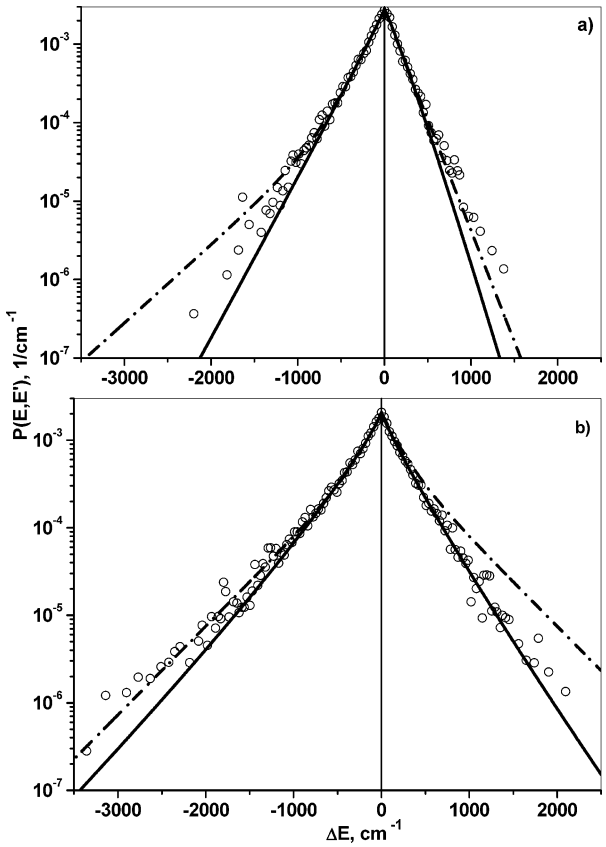

Figure 7. $P(E,E')$ of benzene−Ar collisions at (a) 300 K and (b) 500 K and $\epsilon/\Delta t$ = 3.5 cm^{-1}/fs. The excitation energy is 40 700 cm^{-1}. Shown are the best fit to double exponential, eq 1 (− · −), and stretched exponential, eq 2 with n = 1 (—). The lines become progressively more concave and there is a noticeable supercollision tail at high temperatures at the down-collision part.

the vibrational ones, the value of $\langle\Delta E_R\rangle_a$ changes only a little. All in all, it is clear that rotations also play a very important role in CET in polyatomic-inert gas collisions.

In columns 5−10 are listed the cases where vibrations are selectively frozen by increasing the values of the force constants, as described before. We find that when the IP frequencies are frozen, the value of $\langle\Delta E_V\rangle_d$ decreases in a moderate way. Column 5 gives the value of $\langle\Delta E_V\rangle_d$ when the initial value of the internal energy is distributed among the remaining normal modes and column 8 gives it for the case when the amount of energy that would have been in the frozen modes is subtracted from the original value of the internal energy. Again, there is no significant change in the values of $\langle\Delta E_R\rangle_{u,d}$ even though rotational energy plays a larger role than the vibrational energy in the CET process. Freezing the OOP vibrations, as seen from columns 6 and 9, has a dramatic effect inasmuch as the values of $\langle\Delta E_V\rangle_d$ are reduced by as much as 50%. This is an additional evidence of the importance of the OOP modes to the CET process. When the IP and OOP modes are frozen, as shown in columns 7 and 10, the value of $\langle\Delta E_V\rangle_d$ is reduced even further, as expected.

The mass of the bath has no effect on the values of $\langle\Delta E\rangle$. Comparing columns 2 and 11, where the mass of Ar is increased to the value of the benzene molecule, shows that the values of the original CET quantities are not affected by the mass of Ar. So mass is not responsible for the large differences in the values of the CET quantities and the difference in shapes of $P(E,E')$ of the B−B and B−Ar systems. This agrees with the finding of Lim[13] on the toluene−Ar system where reducing the mass of Ar by a factor of 10 did not affect the values of $\langle\Delta E\rangle$.

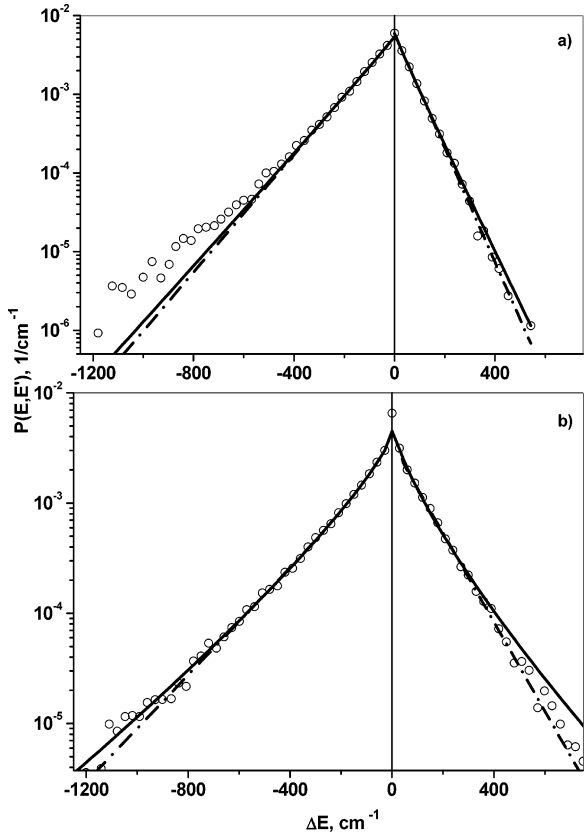

Figure 8. $P(E,E')$ of benzene−Ar collisions at (a) 100 K and (b) 200 K with $\epsilon/\Delta t = 0.35$ cm^{-1}/fs. The excitation energy is 40 700 cm^{-1}. Shown are the best fit to double exponential, eq 1 (− · −), and stretched exponential, eq 2 with $n = 1$ (—). The lines are concave and there is a noticeable supercollision tail at high temperatures at the down-collision part. The peak at $P(0,0)$ is, as expected, sharper than that of Figure 5 but the quantitative features are identical.

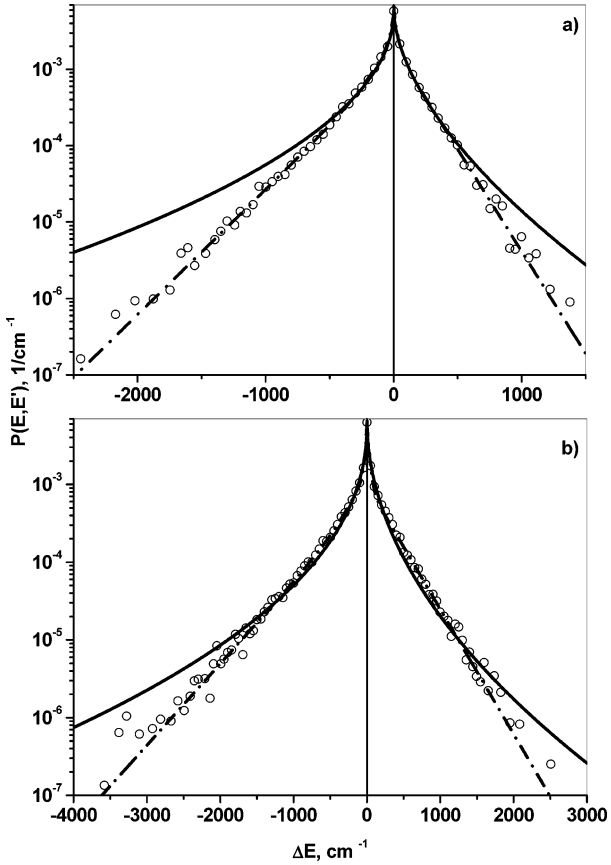

Figure 9. $P(E,E')$ of benzene−Ar collisions at (a) 300 K and (b) 500 K with $\epsilon/\Delta t = 0.35$ cm^{-1}/fs. The excitation energy is 40 700 cm^{-1}. Shown are the best fit to double exponential, eq 1 (− · −), and stretched exponential, eq 2 with $n = 1$ (—). The lines are concave and there is a noticeable supercollision tail at high temperatures at the down-collision part. The peak at $P(0,0)$ is, as expected, sharper than that of Figure 6 but the quantitative features are identical.

Previous findings[21] that indicated that rotations do play a major role in CET in Ar−B find additional support in the present work. Comparing columns 1 in Tables 6 and 7 shows that there is a large change in the value of $\langle\Delta E_V\rangle_a$ when rotations are frozen. This is not surprising because rotations, which play a major role in CET, when frozen, cannot contribute to the down transitions, which are so important to the overall energy transfer. Additional evidence for the essential part that rotations play in CET is provided in the values of the various $\langle\Delta E_V\rangle$'s in columns 2−4 in Table 7 and columns 5−7 in Table 6. Whenever rotations are frozen, the values of the CET parameters are reduced significantly. This is true for each case: frozen IP, frozen OOP, and both IP and OOP frozen. This is contrary to the B−B case where freezing the rotations enhances CET and the values of the various $\langle\Delta E_V\rangle$ increase significantly.

Collisional Energy Transfer Probability Density Function. We have reported previously[23] the CET probability density function for the B−Ar system, and in the present work we repeated the calculations under identical conditions to the B−B system reported above. Figure 6 shows $P(E,E')$ at 100 and 200 K and Figure 7 shows it at 300 and 500 K at $\epsilon/\Delta t = 3.5$ cm^{-1}/fs. As can be seen, the fitting equations, (1) and (2), do a reasonable job at low values of ΔE and deviate at low temperatures and at high values of ΔE. The lines are concave and there is a noticeable supercollision tail[37] at the down-collision part. Figures 8 and 9 show $P(E,E')$ at the same temperatures but with $\epsilon/\Delta t = 0.35$ cm^{-1}/fs. The peak at $P(0,0)$ is, as expected, sharper than that of Figures 6 and 7, but the qualitative features are identical. Y in all the Figures is smaller than unity. It is the smallest at 500 K and increases as the temperature decreases and can reach values larger than unity, i.e., become convex, at low temperatures, as in the case of B−B collisions. The fit of eq 1 is good at all temperatures except the lowest but the stretched exponential does poorly at high values of ΔE, the same as in the B−B system. α, decreases as the temperature increases, again the same as in the B−B case.

Summary and Comparison between B−B Collisions and Ar−B Collisions. The mechanism of energy transfer in polyatomic−polyatomic, PP, collisions differs in principle from that of polyatomic−monatomic, PM, collisions. This is shown clearly in the present, representative, work on B−B and Ar−B collisions. The major channel for energy transfer in PP collisions is V−V transfer, assisted by rotations, whereas in PM it is V−R−T. Large values of ΔE and supercollisions can occur in PP by multiple encounters during the lifetime of the collision complex whereas in PM supercollisions occur when the incoming atom is in phase with an OOP vibration and overall rotations.[18,37] The shape of the down-collisions wing of $P(E,E')$ in PP collisions is convex at low temperatures and becomes a straight line or even slightly concave at higher temperatures. The shape of down-collisions wing of $P(E,E')$ in PM collisions is concave at moderate and high temperatures with a noticeable supercollision tail. The value of $\langle\Delta E\rangle_a$ in PP collisions is much larger than that in a PM collision due to the fact that there is an extra V−V channel that is absent in the latter. The collision complex lifetime has no effect on the value of ΔE in PM collisions because the actual CET event occurs in the last few

tens of femtoseconds of the collision complex lifetime. How long the atom hovers over the polyatomic molecule has no effect on the final outcome. In PP collisions, however, the collision lifetimes do affect the values of ΔE inasmuch as multiple collisions occur, each transferring a given amount of vibrational energy to the cold polyatomic bath. Freezing rotations enhance CET in PP and hinder it in PM.

On the common side, identical and very small net overall rotational energy, $\langle \Delta E_R \rangle_a$, is transferred during the CET but the average values of the up and down CET, $\langle \Delta E_R \rangle_{u,d}$ is large, which indicate active participation of rotation in the energy transfer process. This conclusion is supported by various tests reported above. Also common is the gateway modes for CET. In both cases it proved to be the low-frequency OOP modes of the excited polyatomic molecule. Translational energy transfer values are almost identical, and small, in PP and PM collisions. Even though the average up and down transfer is fairly large, between 100 and 250 cm^{-1}, depending on the temperature, there are equal chances for both events and the net $\langle \Delta E_T \rangle_a$ is small. Though translational energy transfer plays a minor role in PP collisions, V−V, being the major channel, it is the only CET channel in PM collisions, which explains their small $\langle \Delta E \rangle_a$ values.

Acknowledgment. This work is supported by the Technion V. P. R. Fund, by E. And M. Mendelson Research Fund, by the fund for promotion of research at the Technion, and by the Ministry of Science and the Arts under the KAMEA program.

References and Notes

(1) Date, N.; Hase, W. L.; Gilbert, R. G. *J. Phys. Chem.* **1984**, *88*, 5135.
(2) Brown, N. J.; Miller, J. A. *J. Chem. Phys.* **1984**, *80*, 5568.
(3) Bruehl, M.; Schatz, G. C. *J. Phys. Chem.* **1988**, *92*, 7223.
(4) Lendvay, G.; Schatz, G. C. *J. Phys. Chem.* **1990**, *94*, 8864.
(5) Clarke, D. L.; Thompson, E. G.; Gilbert, R. G. *Chem. Phys. Lett.* **1991**, *182*, 357.
(6) Lendvay, G.; Schatz, G. C. *J. Phys. Chem.* **1992**, *96*, 3752.
(7) Clarke, D. L.; Oref, I.; Gilbert, R. G.; Lim, K. F. *J. Chem. Phys.* **1992**, *96*, 5983.
(8) Lendvay, G.; Schatz, G. C. *J. Chem. Phys.* **1992**, *96*, 4356.
(9) Bernshtein, V.; Oref, I. *J. Phys. Chem.* **1993**, *97*, 12811.
(10) Lendvay, G.; Schatz, G. C. *J. Chem. Phys.* **1993**, *98*, 1034.
(11) Lendvay, G.; Schatz, G. C. *J. Phys. Chem.* **1994**, *98*, 6530.
(12) Bernshtein, V.; Oref, I. *J. Phys. Chem.* **1994**, *98*, 3782.
(13) Lim, K. F. *J. Chem. Phys.* (a) **1994**, *100*, 7385; (b) **1994**, *101*, 8756.
(14) Bernshtein, V.; Lim, K. F.; Oref, I. *J. Phys. Chem.* **1995**, *99*, 4531.
(15) Bernshtein, V.; Oref, I. *Chem. Phys. Lett.* **1995**, *233*, 173.
(16) Lenzer, T.; Luther, K.; Troe, J.; Gilbert, R. G.; Lim, K. F. *J. Chem. Phys.* **1995**, *103*, 626.
(17) Koifman, I.; Dashevskaya, E. I.; Nikitin, E. E.; Troe, J. *J. Phys. Chem.* **1995**, *99*, 15348.
(18) Clary, D. C.; Gilbert, R. G.; Bernshtein, V.; Oref, I. *Faraday Discuss.* **1995**, *102*, 423.
(19) Bernshtein, V.; Oref, I. *J. Chem. Phys.* **1996**, *104*, 1958.
(20) Rosenblum, I.; Dashevskaya, E. I.; Nikitin, E. E.; Oref, I. *Mol. Eng.* **1997**, *7*, 169.
(21) Bernshtein, V.; Oref, I. *J. Chem. Phys.* **1997**, *106*, 7080.
(22) Bernshtein, V.; Oref, I. The contribution of Wide Angle Motions to Collisional Energy Transfer Between Benzene and Ar. *ACS Symp. Ser.* **1997**, *678*, 251.
(23) Bernshtein, V.; Oref, I. *J. Chem. Phys.* (a) **1998**, *108*, 3543; (b) **1998**, *109*, 9811.
(24) Yoder, L. M.; Barker, J. R. *J. Phys. Chem. A* **2000** *104*, 10184.
(25) Bernshtein, V.; Oref, I. *J. Phys. Chem. A* **2001**,*105*, 3454.
(26) Bernshtein, V.; Oref, I. *J. Phys. Chem. A* **2001**, *105*, 10646.
(27) Bernshtein, V.; Oref, I. *J. Chem. Phys.* **2003**, *118*, 10611.
(28) Bernshtein, V.; Oref, I. In *Theory of the Dynamics of Elementary Reactions*; Laganà, A.; Lendvay, G., Eds.; NATO Science Series, Kluwer Academic Press, **2004**, *145*, 435.
(29) Bernshtein, V.; Oref, *J. Phys Chem A* **2000,** *104*, 706.
(30) Lenzer, T.; Luther, K. *J. Chem. Phys.* **1996**,*104*, 3391.
(31) Grigoliet, U.; Lenzer, T.; Luther, K. *Z. Phys. Chem.* **2000**,*214*, 1065.
(32) Grigoliet, U.; Lenzer, T.; Luther, K.; Mutzel, M.: Takahara, A. *Phys. Chem. Chem. Phys.* **2001**, *3*, 2191.
(33) Higgins, C. J.; Chapman, S. *J. Phys. Chem. A*, in press.
(34) Hase W. L.; Duchovic R. J.; Hu X.; Komornicki, A.; Lim K. F.; Lu D.-H.; Peslherbe G. H.; Swamy K. N.; Vande-Linde S. R.; Varandas, A.; Wang, H.; Rolf R. J. *QCPE Bull.* **1996**, *16* (4), 43 [QCPE Program 671].
(35) Oref, I.; Tardy, D. C. *Chem. Rev.* **1990**, *90*, 1407.
(36) Hopkins, J. B.; Powers, D. E.; Smalley, R. E. *J Phys. Chem.* **1981**, *85*, 3739.
(37) Oref, I. Supercollisions. In Energy *Transfer from Large Molecules in Nonreactive Systems*; Barker, J. R. Ed.; Advances in Chemical Kinetics and Dynamics Series, Vol. 2B; JAI Press: London, 1995; pp 285−298.
(38) Rossi M. J.; Pladziewicz J. R.; Barker, J. R. *J. Chem. Phys.* **1983**, *78*, 6695.
(39) Shi, J.; Barker, J. R. *J. Chem. Phys.* **1988**, *88*, 6219.
(40) Yerram, M. L.; Brenner, J. D.; King, K. D.; Barker, J. R. *J. Phys. Chem.* **1990**, *94*, 6341.
(41) Toselli, B. M.; Barker, J. R. *J. Chem. Phys.* **1991**, *95*, 8108; **1992**, *97*, 1809.
(42) Barker, J. R.; Brenner, J. D.; Toselli, B. M. *Adv. Chem. Kinet. Dyn.* **1995**, *2b*, 393.
(43) Miller, L. A.; Barker, J. R. J. *Chem. Phys.* **1996**, *105*, 1383.
(44) Damm, M.; Hippler, H.; Olschewski, H. A.; Troe, J.; Wilner, J. *Z. Phys. Chem. (Munich*) **1990**, *166*, 129.
(45) Damm, M.; Deckert, F.; Hippler, H.; Troe, J. J. *Phys. Chem.* **1991**, *95*, 2005.
(46) Damm, M.; Deckert, F.; Hippler, H. *Ber. Bunzen-Ges.* **1997**, *101*, 1901.
(47) Hold, H.; Lenzer, T.; Luther, K.; Reihs, K.; Symonds, A. C. *J. Chem. Phys.* **2000**, *112*, 4076.
(48) Lenzer, T.; Luther, K.; Reihs, K.; Symonds, A. C. *J. Chem. Phys.* **2000**, *112*, 4090.
(49) Sedlacek, A. J.; Weston, R. E.; Flynn, G. W. J. *Chem. Phys.* **1991**, *94*, 6483.
(50) Mullin, A. S.; Michaels, C. A.; Flynn, G. W. *J. Chem. Phys.* **1995**, *102*, 6032.
(51) Michaels, C. A.; Mullin, A. S.; Park, J.; Chou, J. Z.; Flynn, G. W. *J. Chem. Phys.* **1998**, *108*, 2744.
(52) Sevy, E. T.; Rubin, S. M.; Lin, Z.; Flynn, G. W. *J. Chem. Phys.* **2000**, *113*, 4912.
(53) Wall, M. C.; Mullin, A. S. *J. Chem. Phys.* **1998**, *108*, 9658.
(54) Wall, M. C.; Lemoff, A. E.; Mullin, A. S. *J. Chem. Phys.* **1999**, *111*, 7373.
(55) Dashevskaya, E. I.; Nikitin, E. E.; Oref, I. *J. Phys. Chem.* **1993**, *97*, 9397.
(56) Dashevskaya, E. I.; Nikitin, E. E.; Oref, I. *J. Phys. Chem.* **1995**, *99*, 10797.
(57) Rosenblum, I.; Dashevskaya, E. I.; Nikitin, E. E.; Oref, I. *Mol. Eng.* **1997**, *7*, 169.
(58) Dashevskaya, E. I.; Kunc, J. A.; Nikitin, E. E.; Oref, I. *J. Chem. Phys.* **2003**, *118*, 3141.
(59) Nilsson, D.; Nordholm, S J. *Chem. Phys.* **2003**, *119*, 11212.
(60) Bernshtein, V.; Oref, I.; Lendvay, G. *J. Phys. Chem.* **1997**, *101*, 2445.
(61) Lenzer, T.; Luther, K. *Phys. Chem. Chem. Phys.* **2004**, *6*, 955.
(62) Miller, L. A.; Cook, C. D.; Barker, J. R. *J. Chem. Phys.* **1996**,*105*, 3012.